Contents lists available at ScienceDirect

Chemical Engineering Research and Design

journal homepage: www.elsevier.com/locate/cherd

Pressure drop and holdup predictions in horizontal oil–water flows for curved and wavy interfaces

*Lawrence C. Edomwonyi-Otu, Panagiota Angeli**

Department of Chemical Engineering, University College London, Torrington Place, London WC1E 7JE, UK

ABSTRACT

In this work a modified two-fluid model was developed based on experimental observations of the interface configuration in stratified liquid–liquid flows. The experimental data were obtained in a horizontal 14 mmID acrylic pipe, for test oil and water superficial velocities ranging from 0.02 m/s to 0.51 m/s and from 0.05 m/s to 0.62 m/s, respectively. Using conductance probes, average interface heights were obtained at the pipe centre and close to the pipe wall, which revealed a concave interface shape in all cases studied. A correlation between the two heights was developed that was used in the two-fluid model. In addition, from the time series of the probe signal at the pipe centre, the average wave amplitude was calculated to be 0.0005 m and was used as an equivalent roughness in the interfacial shear stress model. Both the interface shape and roughness were considered in the two-fluid model together with literature interfacial shear stress correlations. Results showed that the inclusion of both the interface curvature and the equivalent roughness in the two-fluid model improved its predictions of pressure drop and interface height over the range of studied superficial oil and water velocities. Compared to the two-fluid model with other interfacial shear stress correlations, the modified model performed better particularly for predicting pressure drop.

Keywords: Liquid–liquid flow; Curved interface; Interfacial waves; Interfacial roughness; Two-fluid model; Conductivity probes

1. Introduction

The maturing nature of oil wells increases the amount of water extracted, with water often added in the down-hole to enhance production. Oil–water mixtures need, therefore, to be transported over long distances. The prediction of the two-phase mixture flow properties poses a challenging task because of their dependence on several interrelated factors such as Reynolds number, pipe diameter and inclination among others. An accurate prediction of the pressure drop and holdup is needed for an effective design and maintenance of the fluid transport systems (Hadžiabdić and Oliemans, 2007; Rodriguez and Baldani, 2012). For separated flows the one-dimensional two-fluid model (Taitel and Dukler, 1976; Brauner and Moalem, 1992a) has been used to predict the pressure drop and liquid holdup. Its effectiveness has been found to depend on the closure relations for the wall (oil and water) and interfacial shear stresses as well as the nature of the interface geometry.

In particular, interfacial waves in multiphase flows, which are known to contribute to the observed frictional drag, have not been fully accounted for in the two-fluid model (Andritsos and Hanratty, 1987; Andritsos et al., 2008; Brauner and Moalem, 1993; Brauner et al., 1998; Brauner, 2002; Hadžiabdić and Oliemans, 2007). Although the use of the one-dimensional two-fluid model has yielded some success even in commercial simulators, its ineffectiveness has also been well documented. Rodriguez and Baldani (2012) gave a detailed compendium of the works done so far. Their two-fluid model which included a correlation for the interface curvature and a modified interfacial friction factor based on experimental liquid–liquid flow data and computational fluid dynamic simulations, was able to predict well their experimental results with heavy oil (viscosity of 280 mPas) and water as well as data from other works.

In most of the cited literature, the focus has been on large pipes with internal diameter greater than 20 mm while in recent years there is a growing number of papers on liquid–liquid flows in very small pipes driven by process intensification requirements (Kim and Mudawar, 2012; Tsaoulidis et al., 2012). However, reported data on intermediate pipe sizes (10–20 mmID) are very few in the open literature (Jin et al., 2013; Xu et al., 2010). The flow properties and geometry at

* *Corresponding author*. Tel.: +44 (0) 20 7679 3832.
E-mail address: p.angeli@ucl.ac.uk (P. Angeli).
Received 20 July 2013; Received in revised form 21 May 2014; Accepted 6 June 2014
Available online 13 June 2014
http://dx.doi.org/10.1016/j.cherd.2014.06.009

Nomenclature

Roman symbols

A_o and A_w	area occupied by oil and water phases
dp/dz	pressure gradient (Pa/m)
D_o and D_w	hydraulic diameter of oil and water phases
H_o and H_w	holdup of oil and water phases
h_w	interface height
m	flow regime constant
n	flow regime constant
Re	Reynolds number
Uso and Usw	superficial oil velocity and water velocity

Greek symbols

β	angle in Fig. 7
Δ	delta
γ	proportionality constant in Eq. (16)
α	pipe inclination angle
τ	Shear stress

Subscripts

c, i, o, w	annular core phase, interfacial, oil and water, respectively

these intermediate sizes are known to be greatly influenced by surface and interfacial forces, which become more significant as the diameter reduces, particularly for Eötvös number (E_o, ratio of buoyancy to surface tension forces) greater than 1.0 (Brauner and Moalem, 1992b; Das et al., 2010).

In the present work new experimental data of interface curvature and waviness are presented for separated oil–water flows in a 14 mmID horizontal acrylic pipe. Modifications are suggested to the one-dimensional two-fluid model based on these experimental data. The results of the modifications, particularly to the interface curvature and interfacial shear stress, are compared against predictions obtained when using other interfacial shear stress models available in literature.

2. The one-dimensional two-fluid model for liquid–liquid flows

The one-dimensional two-fluid model (2FM) (Al-Wahaibi and Angeli, 2007; Al-Wahaibi et al., 2007; Brauner and Moalem, 1992a; Taitel and Dukler, 1976) is based on momentum balance equations. Two continuous fluids are considered to flow in layers in a circular pipe according to their density and assumed to be separated by a smooth and flat interface. For a fully developed steady state flow, the integral forms of the one-dimensional momentum equations for the two phases are given by:

$$-A_o\left(\frac{dp}{dz}\right) - \tau_o S_o \mp \tau_i S_i + \rho_o A_o \sin\alpha = 0 \quad (1)$$

$$-A_w\left(\frac{dp}{dz}\right) - \tau_w S_w \pm \tau_i S_i + \rho_w A_w \sin\alpha = 0 \quad (2)$$

The subscripts i, o and w stand for interfacial, oil and water, respectively. S_i, S_o, S_w, A_o and A_w are respectively the perimeters and areas of the phases. By equating the pressure drop in the two phases, the following equation is derived where α (the pipe inclination) is zero for horizontal flow:

$$-\frac{\tau_w S_w}{A_w} + \frac{\tau_o S_o}{A_o} + \tau_i S_i\left(\frac{1}{A_w} + \frac{1}{A_o}\right) = 0 \quad (3)$$

τ_w, τ_o, τ_i are the water wall, oil wall and interfacial shear stresses, respectively. Table 1 shows the geometric parameters used in the two-fluid model.

Table 1 – Geometric parameters used in the two-fluid model.

Parameters (flat interface)	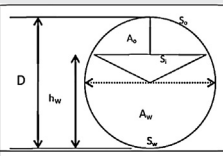
Interfacial length (S_i)	$D\times\left(1-\left(\frac{2h_w}{D}-1\right)^2\right)^{0.5}$
Wall wetted perimeter of the oil phase (S_o)	$D\times\cos^{-1}\left(\frac{2h_w}{D}-1\right)$
Wall wetted perimeter of the water phase (S_w)	$\pi D - S_o$
Cross sectional area of the pipe (A)	$\frac{\pi D^2}{4}$
Area oil phase (A_o)	$\frac{D}{4}\times\left(S_o - S_i\times\left(\frac{2h_w}{D}-1\right)\right)$
Area water phase (A_w)	$A_w = A - A_o$
Oil hold-up (H_o)	$\frac{A_o}{A}$
Water hold-up (H_w)	$\frac{A_w}{A}$
In-situ oil velocity (U_o)	$\frac{U_{so}}{H_o}$
In-situ water velocity (U_w)	$\frac{U_{sw}}{H_w}$

The wall shear stresses, τ_w and τ_o are expressed in terms of the corresponding fluid friction factors, f_w and f_o:

$$\tau_w = \frac{f_w \rho_w U_w^2}{2};\ f_w = mRe_w^{-n} = m\left(\frac{D_w U_w \rho_w}{\mu_w}\right)^{-n} \quad (4)$$

$$\tau_o = \frac{f_o \rho_o U_o^2}{2};\ f_o = mRe_o^{-n} = m\left(\frac{D_o U_o \rho_o}{\mu_o}\right)^{-n} \quad (5)$$

The friction factors are Fanning type and the pipes are considered smooth. The coefficient m and the exponent n are equal to 0.046 and 0.2 respectively for turbulent flow, while 16 and 1.0 are used for laminar flow. D_w and D_o are the hydraulic diameters. Their values are based on the relative velocities of the two phases, which unlike gas–liquid flows are not necessarily different.

$$D_w = \frac{4A_w}{S_w + S_i};\ D_o = \frac{4A_o}{S_o} \text{ for } U_w > U_o \quad (6)$$

$$D_o = \frac{4A_o}{S_o + S_i};\ D_w = \frac{4A_w}{S_w} \text{ for } U_w < U_o \quad (7)$$

$$D_o = \frac{4A_o}{S_o};\ D_w = \frac{4A_w}{S_w} \text{ for } U_w \approx U_o \left(0.98 \le \frac{U_o}{U_w} \le 1.05\right) \quad (8)$$

The parameters S_i, S_o, S_w, A_o and A_w are defined in Table 1. The interfacial shear stress is given by:

$$\tau_i = \frac{f_i \rho_i (U_o - U_w)\,|U_o - U_w|}{2};\ f_i = mRe_i^{-n} = m\left(\left(\frac{S_i}{\pi}\right)\left(\frac{U_i \rho_i}{\mu_i}\right)\right)^{-n} \quad (9)$$

where

$$\rho_i, U_i, \mu_i = \begin{cases} \rho_w, U_w, \mu_w \text{ if } U_w > U_o \\ \rho_o, U_o, \mu_o \text{ if } U_w < U_o \end{cases} \quad (10)$$

When the ratio of the two phase velocities is between 0.98 and 1.05 (Brauner and Moalem, 1992a,b) then there is no interfacial shear stress and both phases are assumed to flow as in an open channel. In this case, the hydraulic diameters are calculated by Eq. (8). By substituting Eq. (4) and (5) in Eq. (1) or Eq. (2), and eliminating $\tau_i S_i$, an expression for the pressure drop of the liquid–liquid system in a horizontal pipe is obtained:

$$\frac{dp}{dz} = \frac{-\tau_w S_w - \tau_o S_o}{A} \tag{11}$$

where A is the cross sectional area of the pipe as defined in Table 1, $A = (A_w + A_o)$. The model is solved iteratively as follows. The pressure drops for the two phases: oil (dp_o/dz) and water (dp_w/dz) are calculated for different interface heights from Eqs. (12) and (13) and the height where the difference between the two pressure drops is zero or almost zero is taken as the solution.

$$\frac{dp_o}{dz} = \frac{\tau_o S_o + \tau_i S_i}{-A_o} \tag{12}$$

$$\frac{dp_w}{dz} = \frac{\tau_w S_w - \tau_i S_i}{-A_w} \tag{13}$$

2.1. Interfacial shear stress correlations

The inclusion of an appropriate interfacial shear stress correlation in the two-fluid model is expected to improve the predictions of pressure drop and water holdup against the experimental results. Arirachakaran et al. (1989) suggested that pressure gradient could be obtained from the sum of the single phase water and oil wall shear stresses averaged over the wall perimeter wetted by each phase. This procedure yielded pressure gradients that were in good agreement with experimental data at low oil and water superficial velocities where the flow was stratified with smooth interface and no slip between the phases existed. This implied that the interfacial shear stress (τ_i) could be neglected. Brauner (1991) proposed the following correlation for the interfacial friction factor f_i, for annular liquid–liquid flows where the faster flowing phase forms the core:

$$f_i = Bm\left(\frac{D_c U_c \rho_c}{\mu_c}\right)^{-n} \tag{14}$$

The interfacial shear stress τ_i is calculated from:

$$\tau_i = f_i\left(\frac{\rho_c U_c^2}{2}\right) \tag{15}$$

Here, D_c, μ_c, ρ_c, U_c are respectively the diameter, viscosity, density and average velocity of the core phase, B is an augmentation factor that accounts for interfacial waviness, while n and m are the constants in the friction factor-Reynolds number correlation. The value of B varies between 0.8 and 1 (Neogi et al., 1994), although Brauner (1991) suggested that B should be taken equal to 1 as a result of the slight waviness of the liquid–liquid interface. Hall (1992) suggested that for flow between parallel plates, the oil wall shear stress is related to the interfacial shear stress by a proportionality factor γ, closely related to the water/oil viscosity ratio. This factor was calculated from the analytical solution of the one-dimensional momentum equations for oil–water stratified laminar flow between parallel plates. The factor γ should be less than unity since the oil phase is almost always more viscous than the water phase. According to Hall (1992) τ_i is given by:

$$\tau_i = \gamma \tau_o \tag{16}$$

where τ_o is the oil wall shear stress.

According to Taitel et al. (1995), the interfacial friction factor should be equal to 0.0142, unless the wall friction factor of any of the phases becomes larger than this value, in which case the larger value should be used.

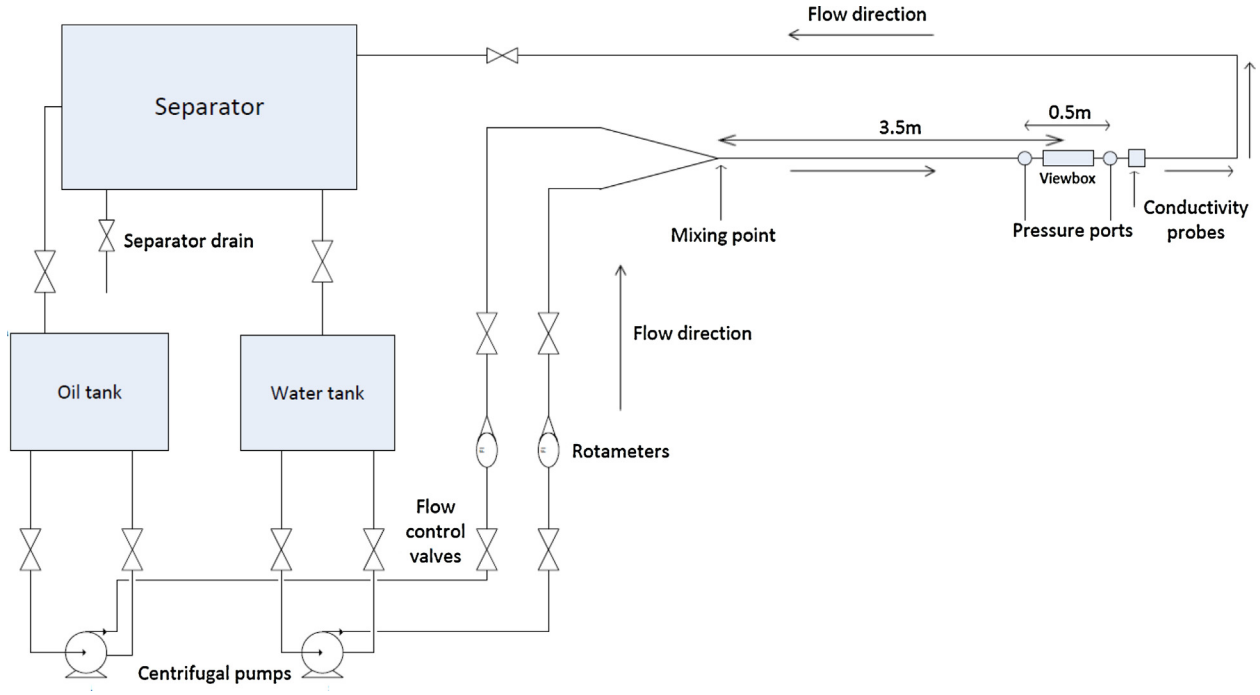

Fig. 1 – Schematic of the experimental oil–water flow facility.

Table 2 – Properties of test fluids.

	Water	Oil
Density	$\rho_w = 1000\,kg/m^3$	$\rho_o = 828\,kg/m^3$
Viscosity	$\mu_w = 1\,mPa\,s$ at 23 °C	$\mu_o = 5.5\,mPa\,s$ at 23 °C
Oil–water interfacial tension	39.6 mN/m at 23 °C	

3. Experimental setup

The test fluids used in this investigation are tap water and a model oil (EXXSOL D140, Exxon Chemicals). Their properties are shown in Table 2. The experiments were performed in the liquid–liquid flow facility shown in Fig. 1. The fluids from their respective storage tanks are fed separately to the test section via fixed flowrate centrifugal pumps (Procon, Sandtex; 12 l/min, 300 kPa). Recycle loops are used to regulate the flowrates which are measured with variable area flowmeters, one for each fluid, that are located after the pumps. The maximum flowrate is 7.5 l/min for both oil and water flows. The flowmeters were calibrated for each fluid and found to have an uncertainty of 0.013 l/min. The fluids are brought together at the beginning of the test section via a smooth Y-junction with a very small angle that ensures minimum mixing. The test section is a 14 mmID, 4 m long acrylic pipe made up of shorter lengths joined together with flanges that allow instrumentation to be placed at different distances from the inlet. After the test section the fluids return via an acrylic pipe with 14 mmID to a gravity separator vessel and they eventually flow back to their respective tanks after separation. The water can be drained directly from the separator if no longer needed for further runs. A view box, filled with glycerol, is placed 3.5 m downstream the inlet for flow visualization. Flow patterns were recorded for superficial oil (Uso) and water (Usw) velocities ranging from 0.008 m/s to 0.58 m/s and from 0.05 m/s to 0.8 m/s, respectively, with a high speed camera (Photron Ultima APX (monochrome) at 1200 fps, positioned opposite the acrylic viewing box. Images were taken after about 600 s once the flow was started to avoid any start up effects. Pressure drop was measured through two pressure taps, 0.5 m apart, located before and after the viewing box, by a differential pressure transducer (ABB 266MST; max pressure 6 kPa, 0.04% base scale accuracy).

Two conductivity probes, a ring and a wire, were located 0.1 m after the viewing box. They were used to measure the oil–water interface heights. The wire probe consists of two parallel wires 4 mm apart, stretched along a vertical pipe diameter (see Fig. 2). This probe provides a measurement of interface height over time in the middle of the pipe

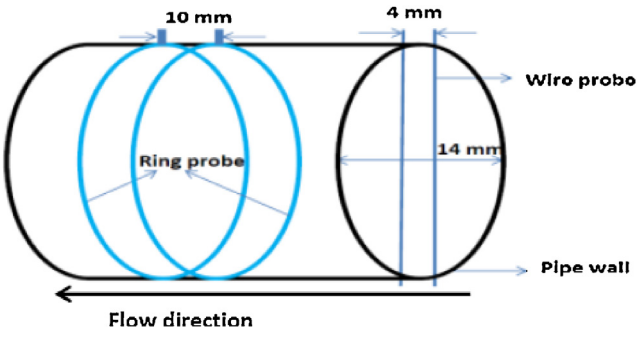

Fig. 2 – Schematic of the arrangement of the two conductivity probes.

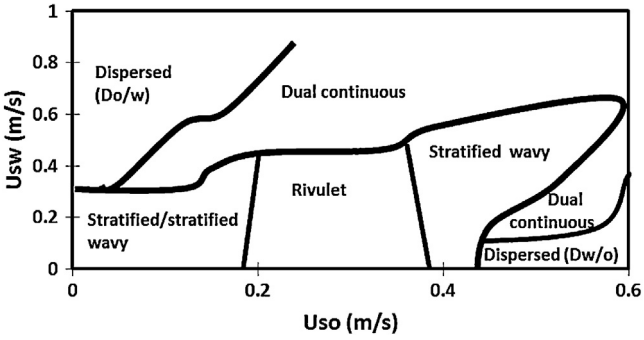

Fig. 3 – Flow pattern map for the oil–water flow in the 14 mmID horizontal acrylic pipe.

cross-section. The ring probe consists of two metallic rings which are embedded at the circumference of the pipe, flush with the internal wall and in contact with the fluids. The rings are 3 mm wide and 10 mm apart (Fig. 2). This probe measures the interface height over time next to the wall. For each set of conditions, data was collected from the two probes at a frequency of 512 Hz and for 240 s and then averaged. The probe signals were calibrated and processed to give average interface heights following the procedure given in Barral and Angeli (2013). Pressure drop and interface height measurements were taken in the separated flow regions, for pairs of superficial oil (Uso) and water (Usw) velocities of 0.02–0.51 m/s and 0.05–0.62 m/s, respectively. The experimental results were used in the two-fluid model as a basis for comparing interfacial stress models, and for introducing modifications that take into account the interface shape.

4. Results and discussion

4.1. *Flow patterns*

The flow patterns observed under the flow conditions studied are shown in Fig. 3. Stratified and stratified-wavy flows were observed for a wide range of superficial water and oil velocities. As the phase velocities increased beyond 0.1 m/s, the interface became notably wavy, while the amplitude of the waves increased as the transition to other patterns approached (see Figs. 3 and 4a, b). Results from the conductivity probe indicate that there are always waves present at the interface, which for low velocities are very long with small amplitudes that are not easily observed visually; in these cases the flow in recordings appears as stratified smooth (see for example Fig. 4a).

At $Usw < 0.34$ m/s and $Uso > 0.15$ m/s, rivulet flow (see Figs. 3 and 4c) was observed. The two fluids appear to flow in a helical way along the pipe, following the path of least resistance. Sometimes at around $Uso = 0.2$ m/s and $Usw = 0.1$ m/s to 0.3 m/s, the rivulet flow would change to stratified after a long time. These conditions are in the boundary between the two flow patterns. As the oil velocity further increased for a fixed water velocity, the rivulet flow would become disturbed and change to stratified-wavy at $Uso > 0.39$ m/s. The spiral frequency of the rivulets depended on the difference between the superficial oil and water velocities; for a fixed oil velocity, the frequency reduced with increasing water velocity.

At $Usw > 0.336$ m/s and $Uso > 0.07$ m/s, the pattern was dual continuous (see Figs. 3 and 4d) with drops of each phase into the other. With increasing phase and mixture velocity the number of drops increased but their size decreased. The

Flow patterns	Images
Stratified flow	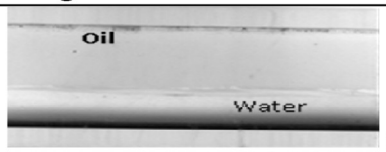 (a)
Stratified wavy flow	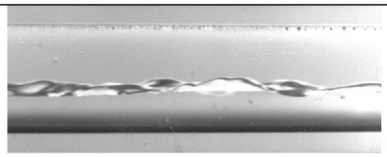 (b)
Rivulet flow	 (c)
Dual continuous flow	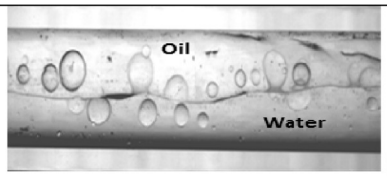 (d)
Dispersed (oil in water)	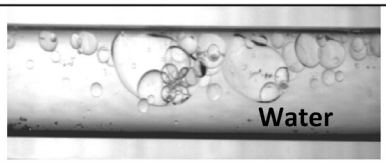 (e)
Dispersed (oil in water)	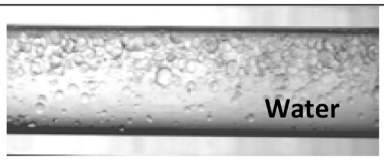 (f)
Dispersed (water in oil)	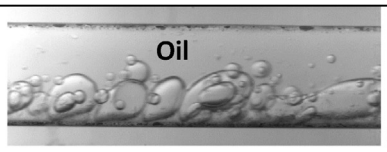 (g)

Fig. 4 – Photographs of the oil–water flow patterns in the 14 mmID horizontal acrylic pipe.

observed sizes ranged from around 0.1*D* to 0.3*D* (where *D* is the pipe internal diameter). Interestingly, when the drops were present there was no significant interfacial waviness.

Dispersed flows were seen at low oil and high water velocities, Uso < 0.2 m/s and Usw > 0.34 m/s (dispersed oil-in-water, Do/w) (see Figs. 3 and 4e) and at low water and high oil velocities Uso > 0.45 m/s and Usw < 0.2 m/s (dispersed water-in-oil, Dw/o) (see Figs. 3 and 4g). In both types of dispersions, the drop size decreased and their number increased as the continuous phase velocity increased which can be observed in Fig. 4e and f. It is interesting to note that within the region of velocities investigated, there were no steady annular and slug flows. They appeared for a short time in between changes in superficial fluid velocities before a new steady state flow was achieved, mainly for Usw from 0.3 m/s to 0.6 m/s and Uso from 0.15 m/s to 0.35 m/s.

The flow patterns observed in this investigation are similar to the results by Xu et al. (2010) who carried out experiments in a 20 mmID horizontal acrylic resin pipe using fluids with similar properties as in this study (water and diesel oil with $\mu_o = 5.5$ mPa s and $\rho_o = 828$ kg/m^3). However, they did not observe any rivulet flow pattern.

Rivulet flows are considered to be unique to pipes of small diameter where surface and interfacial phenomena become important. The Eötvös number for the system used in this work is 4.85, indicating that the pipe can be considered small (Brauner and Moalem, 1992b; Panton and Barajas, 1993). Similarly, Das et al. (2010), observed rivulet flow in a 12 mmID pipe. In their case the pattern was seen at higher superficial water and kerosene velocities than in this investigation, probably as a result of different fluid properties and pipe sizes.

Using the same fluids and test section Al-Wahaibi et al. (2007) observed stratified and dispersed oil-in-water flows at the same superficial velocity ranges as in the current work. However, the region where they observed dual continuous flow was found to be stratified wavy in this study. Al-Wahaibi et al. (2007) also found annular flow at high fluid velocities (Usw > 0.6 m/s and Uso > 0.35 m/s) in the same region where dual continuous flow is seen in this work but did not report rivulet and dispersed water-in-oil flows. In addition, they recorded steady slug flow at Uso = 0.16–0.33 m/s and Usw > 0.6 m/s where the transient slug flow and upper boundary of dispersed oil-in-water (Do/w) flow appear in the current work. The differences could be due to the inlet geometries

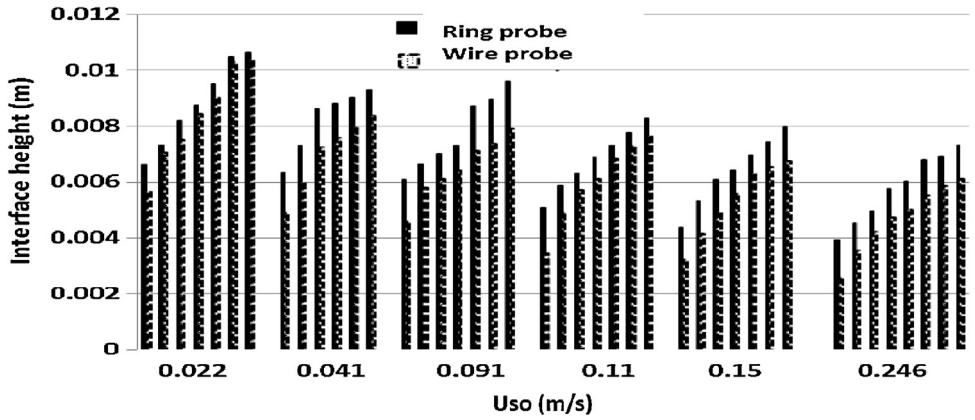

Fig. 5 – Comparison of interface heights from the two conductivity probes at different superficial oil velocities for superficial water velocities Usw = 0.052, 0.11, 0.166, 0.22, 0.28, 0.336, 0.393 and 0.45 m/s, respectively from left to right.

used in the two studies; in Al-Wahaibi et al. (2007) a Y-inlet was used that had a wider angle than the inlet used in the current work.

4.2. *Modifications to the two-fluid model*

In what follows, only data within the separated regions (stratified, stratified wavy and rivulet) are used to compare against the two-fluid models. The experimental results on average interface height from the two probes are shown in Fig. 5. As can be seen the average interface height at the wall (given by the ring probe) is always higher than in the middle of the pipe (given by the wire probe), suggesting a curved interface shape with a concave geometry. Based on all the data collected, it was found that the interface height at the wall, h_w, and the interface height in the middle of the pipe, h_b, can be related as follows:

$$h_b = \frac{1.065 h_w D}{0.014} - 0.0009 \quad (17)$$

where D, h_w and h_b are measured in meter (m).

The experimental interface heights from both probes are compared against the predictions of the standard two-fluid model (2FM) in Fig. 6. As can be seen, there is reasonable agreement between predictions and experiments, particular for the data from the ring probe. This is reflecting the importance of the wall wetted perimeters on the calculation of shear stresses in the two-fluid model. The model gives higher interface heights than the experimental ones, apart from superficial water velocities, Usw, below 0.16 m/s; for these velocities the

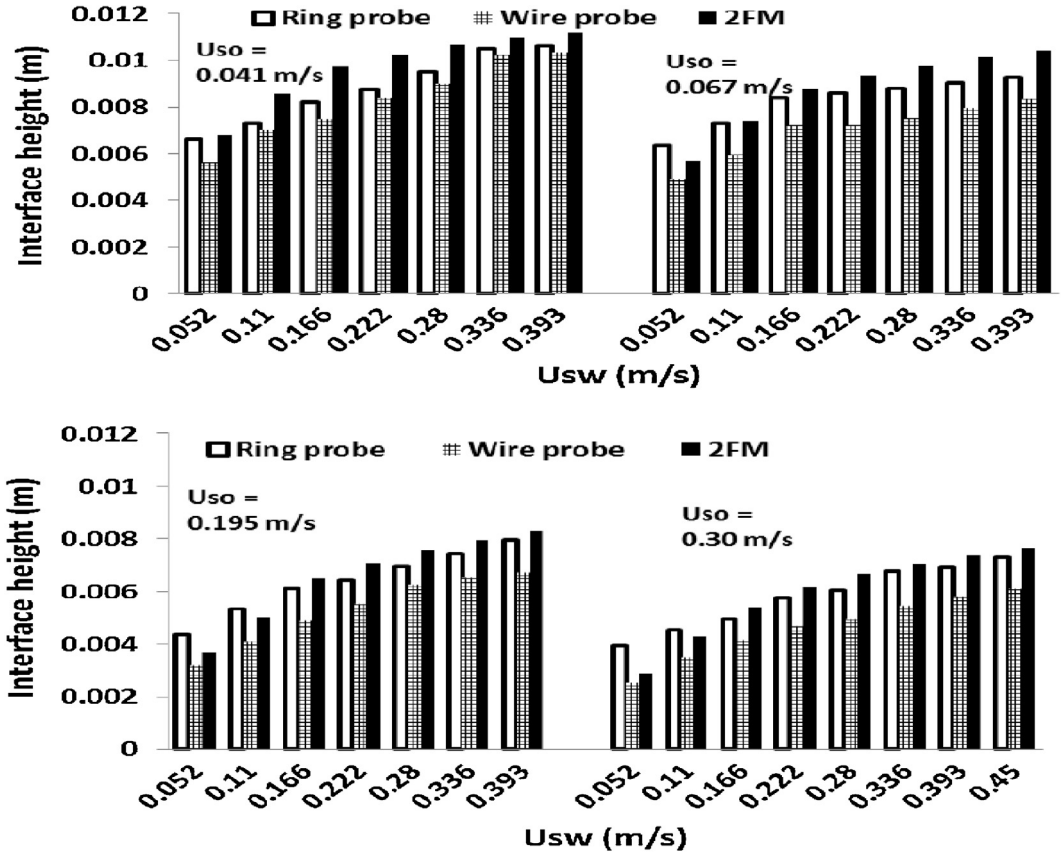

Fig. 6 – Comparison of the experimental interface heights from the two conductivity probes with the predictions of the two-fluid model for different superficial oil and water velocities.

predictions are in fact closer to the data from the wire probe. The change from under- to over-prediction at Usw > 0.11 m/s coincides with the change in the friction factor constants used for the water phase, from the laminar to the turbulent values. At Usw < 0.16 m/s the Reynolds numbers for water lie between 1600 and 2600 but in the model the friction factor constants for laminar flow are used. In these conditions the oil phase is clearly laminar with Reynolds numbers below 1600. The model predictions agreed better with the experimental data when a Reynolds number of 1500 instead of 2100 was used for the transition from laminar to turbulent flow.

The interface height time series data from the probes show that there are always waves at the interface even at low phase velocities. It has been suggested that waves can be considered as interfacial roughness and should be included in the interfacial shear stress term of the two-fluid model (De Castro et al., 2012; Hadžiabdić and Oliemans, 2007). From the time series data of the wire probe, the interfacial waves were found to have average amplitude of 0.0005 ± 0.0002 m for the range of velocities studied. This value was used as roughness in the interfacial friction factor correlation proposed by Rodriguez and Baldani (2012):

$$f_i = f_k \left[1 + C_i \frac{\alpha}{D}\right] \quad (18)$$

where C_i is a correction factor taken as 50 (Rodriguez and Baldani, 2012), α is the interfacial wave amplitude and f_k is the wall friction factor of the faster phase.

4.2.1. *Geometric parameters of the two-fluid model with curved interface*

The two-fluid model described in Section 2 was modified to account for the interface curvature found experimentally. A schematic showing the geometric parameters of the stratified oil–water flow with curved interface is given in Fig. 7. R is the radius of the circle with center C which gives the appropriate interface curvature. The various geometric parameters needed for the two-fluid model when the interface is curved are calculated as follows:

$$\text{Wall wetted perimeter of the oil phase, } S_o = D \times \text{Cos}^{-1}\left(\frac{2h_w}{D} - 1\right) \quad (19)$$

$$\text{Wall wetted perimeter of the water phase, } S_w = \pi \times D - S_o \quad (20)$$

$$\text{Interfacial length, } Si = \beta \times R \quad (21)$$

$$\text{Area of oil phase, } A_o = 0.5(S_i \times R - R^2 \text{Sin}\,\beta) + 0.25D \times S_o - 2X(2h_w - D) \quad (22)$$

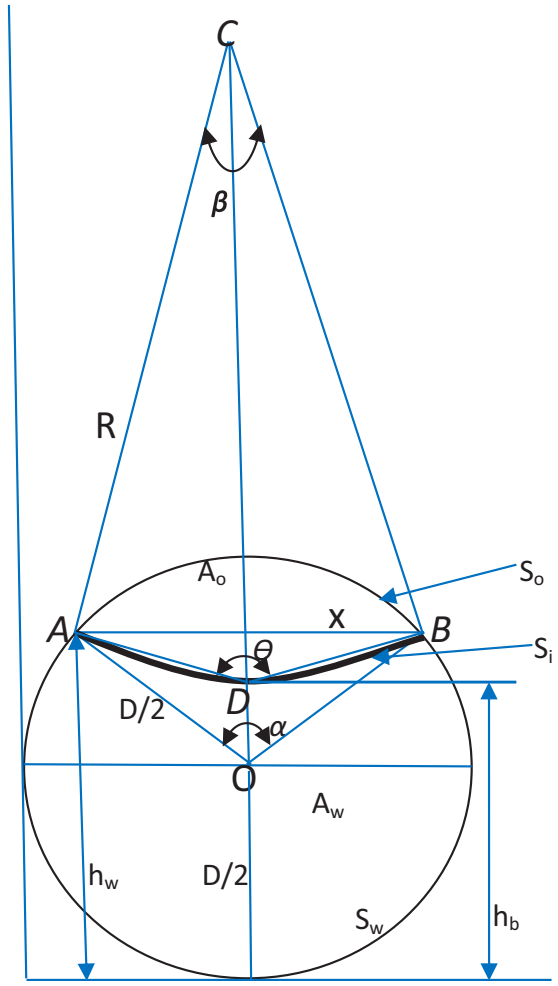

Fig. 7 – Geometric parameters used in the two-fluid model with curved interface. The thick curved line within the circle represents the curved interface.

$$\text{Area of water phase, } A_w = 0.25\pi \times D^2 - A_0 \quad (23)$$

Eqs. (19)–(23) are used to calculate the other parameters of the two-fluid model as shown in Section 2. As can be seen, only the interfacial length (Si) and the area of the phases are directly affected by the inclusion of the curved interface. Table 3 shows the pressure drop data obtained experimentally in the separated flow regions.

Table 3 – Pressure drop (Pa/m) for startified/stratified wavy oil–water flow obtained in the 14 mmID acrylic pipe.

*Usw (m/s)	+Uso (m/s)						
	0.022	0.067	0.11	0.195	0.3	0.432	0.51
0.052	40	70	100	120	360	440	–
0.11	60	90	140	180	300	480	–
0.166	80	110	180	220	370	540	–
0.222	110	150	210	280	480	620	–
0.28	140	180	250	320	500	720	800
0.336	180	240	300	380	570	740	840
0.393	–	–	–	460	640	820	920
0.45	–	–	–	500	720	920	1020
0.51	–	–	–	–	–	1040	1160
0.563	–	–	–	–	–	1160	1280
0.62	–	–	–	–	–	–	1380

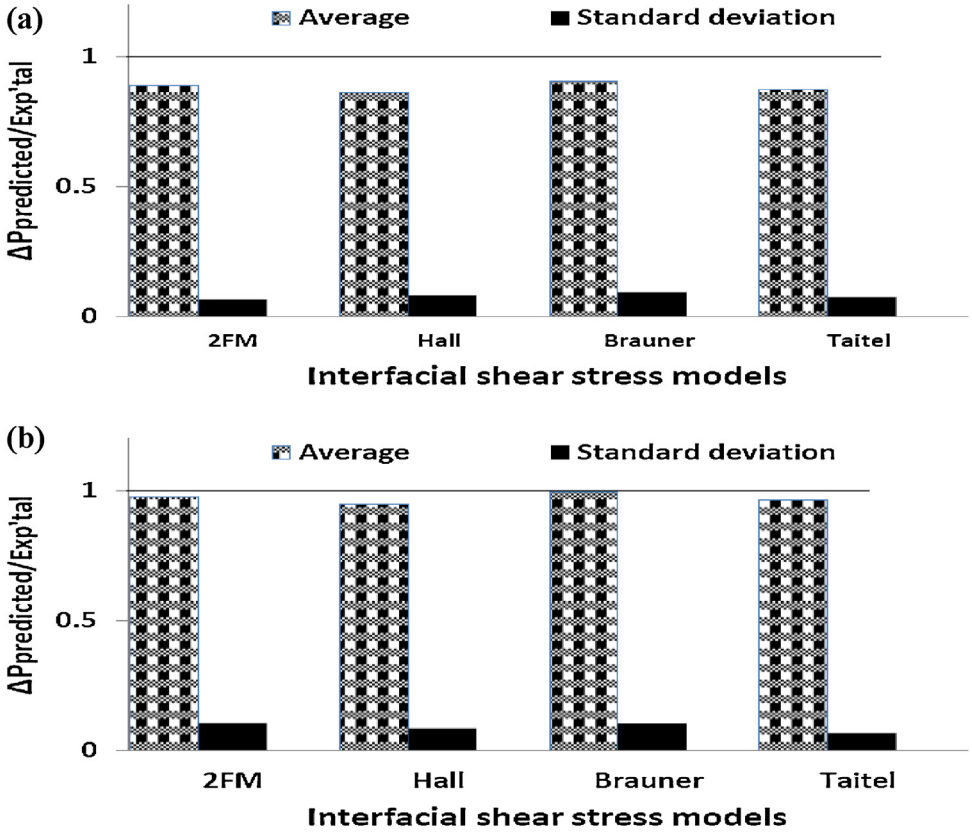

Fig. 8 – Comparison of experimental pressure drop values averaged over all data shown in Table 3 against the ones predicted from the two-fluid model using different interfacial shear stress correlations. Constants in Eq. (4) are (a) $m = 0.046$, $n = 0.2$ (b) $m = 0.0792$, $n = 0.25$.

4.3. *Predictions of two-fluid model with different interfacial shear stress correlations*

The experimental data on pressure drop within the separated flow regions (see Table 3) are compared in Fig. 8 against the predictions of the standard two-fluid model with different interfacial shear stress correlations (Brauner, 1991; Hall, 1992; Taitel et al., 1995; see Section 2.1). Different values of the friction factor-Reynolds number correlation constants (Eqs. (4) and (5)) for turbulent flow were used with $m = 0.046$, $n = 0.2$ in Fig. 8a and $m = 0.0792$, $n = 0.25$ (Blasius correlation) in Fig. 8b, respectively.

As can be seen, the values of the friction factor-Reynolds number constants affect the pressure drop predictions with the Blasius constants giving better results. The constants used for Fig. 8a are suitable for Reynolds numbers greater than 10^5, while the Blasius equation (Fig. 8b) is recommended for Reynolds numbers between 2500 and 10^5. In fact, the phase Reynolds numbers for the conditions investigated were below 10^5. Based on the improved predictions, the Blasius correlation will be used for further calculations. From the various interfacial stress models, the standard two-fluid model (2FM) agreed better with the experimental data in Fig. 8a, while the models by Brauner (1991) and Taitel et al. (1995) gave better predictions in Fig. 8b in terms of average value and standard deviation, respectively.

4.4. *Predictions of the modified two-fluid model*

The average predictions of the two-fluid model (2FM) on pressure drop, including the effects of interfacial waviness and interface curvature are shown in Fig. 9. The effects of interface roughness (model 2FM + R) and of interface curvature (2FM + CI) are considered separately initially and are then combined in the 2FM + R + CI model. As can be observed, the interfacial roughness and curvature do not seem to improve the average pressure drop values. In the small pipe used in this work and for the range of conditions where separated flows were obtained, the amplitude of the interfacial waves was quite small (generally less than 1 mm), and their contribution to interface roughness (2FM + R model) does not seem to be significant. When the interface curvature was included (2FM + CI), the average pressure drop prediction did not improve but the standard deviation decreased, indicating that the model was able to predict the pressure drop better across all the mixture velocities compared to 2FM. By combining both effects of interface roughness and curvature (2FM + R + CI), the standard deviation reduced by almost 50%. The improvements were mainly observed at low water velocities, where the

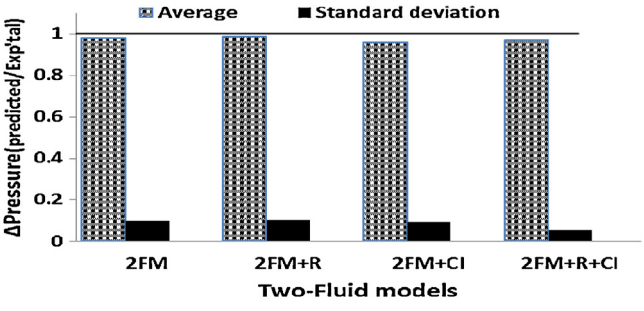

Fig. 9 – Comparison of experimental pressure drop values averaged over all data shown in Table 3 against the ones predicted from the two-fluid model using interface roughness and interface curvature.

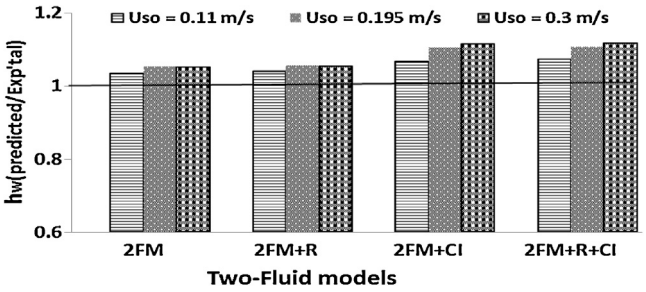

Fig. 10 – Comparison of experimental interface heights at the wall against the ones predicted from the two-fluid model using interface roughness and interface curvature. For each superficial oil velocity, heights are averaged over all corresponding superficial water velocities shown in Table 3.

interface curvature is generally more pronounced as can be seen from the experimental data (Figs. 5 and 6). In general, for a fixed Uso the relative difference between the interface heights, measured from both probes, diminishes with increasing Usw.

Predicted interface heights are compared against the experimental ones in Fig. 10 using the models described above. The interface heights at the wall, h_w, are used which were found to be closer to the predictions of the standard two-fluid model than those in the middle of the pipe (see Fig. 6). Clearly, in all cases the interface height is over-predicted and in fact the modifications of the two-fluid model either do not change significantly or even deteriorate the predictions, particularly with the inclusion of the curved interface.

The prediction of the interface height (h_b) at the middle of the pipe, obtained from the model with curved interface, follows a similar trend of over-prediction. This follows from the linear relationship shown in Eq. (17).

4.5. *Predictions of the modified two-fluid model with literature correlations on interfacial shear stress*

The effects of different interfacial shear stress correlations on the predictions of pressure drop by the two-fluid model are considered here. In all cases the interface is assumed to be curved. Interface roughness associated with waves, as given by Eq. (18), is taken into account in the 2FM + R + CI model. As can be seen from Fig. 11 the model by Brauner (1991) with curved interface (Brauner + CI) gives the best absolute prediction of the average pressure drop of about 99 ± 11%, while the model proposed in this work (2FM + R + CI) gives a good prediction with the lowest standard deviation of 5% (97 ± 5%).

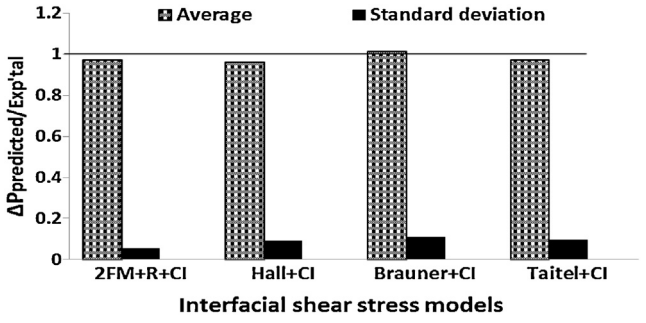

Fig. 11 – Comparison of experimental pressure drop values averaged over all data shown in Table 3 against the ones predicted from the two-fluid model with curved interface using different interfacial shear stress correlations.

Both these models considered interface waviness. In the current model this is included as roughness while in the Brauner (1991) model it is accounted for in the augmentation factor B. The predictions of the other two models, Hall (1992) and Taitel et al. (1995) are not as good. In both these models the interfacial shear stress is taken as constant (ratio of fluid viscosities for the Hall model and a constant value of 0.0142 for the Taitel model). In fact, in the Hall model the predictions improved with superficial water velocity, while in the Taitel model the predictions were better at low superficial oil velocities than at high ones. It should be noted here that considering interface curvature did not improve the predictions of the two-fluid model with the literature interfacial shear stress terms either in terms of average value or standard deviation (compare Fig. 11 with Fig. 8b). A curved interface, however, decreased significantly the standard deviation in our model when combined with interface roughness (Fig. 9).

Furthermore, the model proposed here was compared against the one recently proposed by Rodriguez and Baldani (2012), which also included interface curvature and waviness. In addition, the model suggested a modified hydraulic diameter of the slower light phase in laminar flow. The model by Rodriguez and Baldani predicted the current experimental data with an accuracy of about 66 ± 8% compared to 97 ± 5% of the current (2FM + R + CI) model. It was observed that the accuracy of their model increased with water velocity for a fixed oil velocity. This under-prediction by the Rodriguez and Baldani model may be due to the modifications of most of the parameters (hydraulic diameters, friction factors and wall shear stresses) compared to those of the traditional two-fluid model (2FM). It was also found that the correlation proposed by Rodriguez and Baldani for interface curvature predicted a concave shape for most of the current data except at very low Usw (0.052 m/s) and for Uso > 0.19 m/s, where it gave a convex interface; in the current work a concave interface shape was found in all cases of stratified flow studied.

The predictions of the interfacial height (h_w) by the different interfacial stress models with and without curved interface are presented in Fig. 12. In all cases, including a curved interface resulted in an increase in the interface height values predicted. Furthermore, it was found that for all models the predicted values were lower than the experimental ones at low superficial oil velocities; as the oil velocity increased the predictions also increased and became higher than the experimental ones. This was more prominent when interface curvature was included. In particular, for Usw < 0.17 m/s the Hall model under-predicted the experimental data by as much as 20–25% but this was improved to 13% when a curved interface was used. Under the same conditions the Brauner model under-predicted the experimental data by 30–35% and was improved to 14% with curved interface. Similarly at these conditions, the Taitel model was improved to 11% with the curved interface added.

Overall, the Hall model with curved interface was the best among the other models with 6% over-prediction of the absolute height and a standard deviation of less than 10%. In comparison, the model suggested in this study (2FM + R + CI) over-predicted the experimental height by about 7% and a standard deviation of 11%.

The two-fluid model with interfacial waviness and curvature of the oil–water interface included predicts satisfactorily both the pressure drop and the interface height with small standard deviation. These finding agree with previous reports which consider interface waviness and curvature

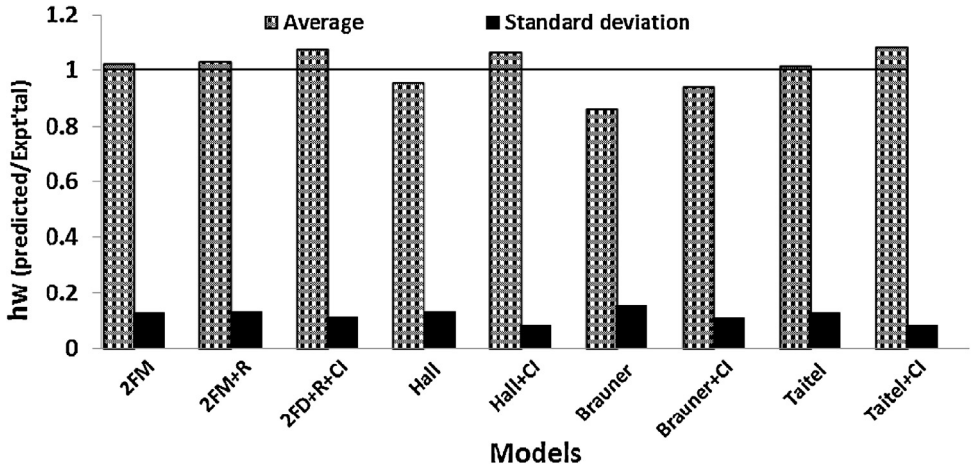

Fig. 12 – Comparison of experimental interface heights at the wall averaged over all data shown in Table 3 against the ones predicted from the two-fluid model using different interfacial shear stress correlations for both flat and curved interface.

important for improving the predictions of the two-fluid model (Andritsos and Hanratty, 1987; Andritsos et al., 2008; Brauner and Moalem, 1993; Brauner et al., 1998; Brauner, 2002; Hadžiabdić and Oliemans, 2007; De Castro et al., 2012; Rodriguez and Baldani, 2012).

5. Conclusions

The significance of pressure drop and holdup in designing an efficient system for oil–water transport necessitates the development of robust predictive models. One of the drawbacks has been the limited availability of experimental data for liquid–liquid flows. In this paper, flow patterns are presented for a wide range of superficial oil and water velocities in a small diameter test section. Particularly for separated flows, new experimental data are given on the interface configuration. The data enabled modifications to the two-fluid model that account for the interface waviness through a roughness factor and for the interface curvature. The modified model showed improved predictive accuracy of over 95% for pressure drop across the range of experimented oil and water velocities, while the interface height was predicted within 90% accuracy. It was found that the predictions of the interface height were particularly sensitive to interface curvature, while those of pressure drop were affected by both the interface roughness and curvature. The results showed that the modified model performed better when compared against the two-fluid model that includes literature interfacial shear stress correlations particularly in predicting the pressure drop.

Acknowledgements

L.C. Edomwonyi-Otu would like to thank the Petroleum Technology Development Fund (PDTF) Nigeria for his studentship. The authors would like to acknowledge the EPSRC Engineering instrument pool for providing the high-speed camera system. The authors are grateful to Dr Simon Barrass for his technical support.

References

Al-Wahaibi, T., Angeli, P., 2007. Transition between stratified and non-stratified horizontal oil–water flows. Part I. Stability analysis. Chem. Eng. Sci. 62, 2915–2928.

Al-Wahaibi, T., Smith, M., Angeli, P., 2007. Effect of drag-reducing polymers on horizontal oil–water flows. J. Pet. Sci. Eng. 57, 334–346.

Andritsos, T., Tzotzi, C., Hanratty, T.J., 2008. Interfacial shear stress in wavy stratified gas–liquid two-phase flow. In: 5th European Thermal-Sciences Conference, The Netherlands, pp. 0–7.

Andritsos, T., Hanratty, T., 1987. Influence of interfacial waves in stratified gas–liquid flows. AIChE J. 33, 444–454.

Arirachakaran, S., Oglesby, K.D., Shoulam, O., Brill, J.P., 1989. An analysis of oil water flow phenomena in horizontal pipes. In: SPE Proceeding: Production Operation Symposium. SPE, pp. 155–167.

Barral, A.H., Angeli, P., 2013. Interfacial characteristics of stratified liquid–liquid flows using a conductance probe. Exp. Fluids 54, 1604:1–15.

Brauner, N., 1991. Two-phase liquid–liquid annula flow. Int. J. Multiph. Flow 17, 59–76.

Brauner, N.,2002. Modelling and control of two-phase phenomena: liquid–liquid two-phase flow systems. In: Modeling and Control of Two-Phase Flow Phenomena. CISM, Udine, Italy.

Brauner, N., Moalem, D., 1992a. Flow pattern transitions in two-phase liquid–liquid flow in horizontal tubes. Int. J. Multiph. flow 18, 123–140.

Brauner, N., Moalem, D., 1992b. Identification of the range of small diameter conduits, regarding two-phase flow pattern transitions. Int. Commun. Heat Mass Transf. 19, 29–39.

Brauner, N., Moalem, M., Rovinsky, J., 1998. A two-fluid model for stratified flows with curved interfaces. Int. J. Multiph. Flow 24, 975–1004.

Brauner, N., Moalem, M.D., 1993. The role of interfacial shear modelling in predicting the stability of stratified two-phase. Chem. Eng. Sci. 48, 2867–2879.

Das, G., De, B., Mandal, T.K., 2010. The rivulet flow pattern during oil–water horizontal flow through a 12 mm pipe. Exp. Therm. Fluid Sci. 34, 625–632.

De Castro, M.S., Pereira, C.C., Dos Santos, J.N., Rodriguez, O.M.H., 2012. Geometrical and kinematic properties of interfacial waves in stratified oil–water flow in inclined pipe. Exp. Therm. Fluid Sci. 37, 171–178.

Hadžiabdić, M., Oliemans, R.V.A., 2007. Parametric study of a model for determining the liquid flow-rates from the pressure drop and water hold-up in oil–water flows. Int. J. Multiph. Flow 33, 1365–1394.

Hall, A.R.W., 1992. Multiphase Flow of Oil, Water and Gas in Horizontal Pipes. University of London, London.

Jin, N., Zhao, A., Zhai, L., Gao, Z., 2013. Liquid holdup measurement in horizontal oil–water two-phase flow by using concave capacitance sensor. In: International Conference on Multiphase Flows (ICMF), Jeju, South Korea, pp. 1–8.

Kim, S.-M., Mudawar, I., 2012. Universal approach to predicting two-phase frictional pressure drop for adiabatic and condensing mini/micro-channel flows. Int. J. Heat Mass Transf. 55, 3246–3261.

Neogi, S., Lee, A., Jepson, W.P., 1994. A model for multiphase (gas–water–oil) stratified flow in horizontal pipelines. In: Proc. SPE Asia Pacific Oil Gas Conf, pp. 553–562.

Panton, R.L., Barajas, A., 1993. The effect of contact angle in two-phase flow in capillary tubes. Int. J. Multiph. Flow 19, 337–346.

Rodriguez, O.M.H., Baldani, L.S., 2012. Prediction of pressure gradient and holdup in wavy stratified liquid–liquid inclined pipe flow. J. Pet. Sci. Eng. 96–97, 140–151.

Taitel, Y., Barnea, D., Brill, J.P., 1995. Stratified three phase flow in pipes. Int. J. Multiph. Flow 21, 53–60.

Taitel, Y., Dukler, A.E., 1976. A model for predicting flow regime transitions in horizontal and near horizontal gas–liquid flow. AIChE J. 22, 47–55.

Tsaoulidis, D., Dore, V., Angeli, P., Plechkova, N.V., Seddon, K.R., 2013. Dioxouranium(VI) extraction in microchannels using ionic liquids. Chem. Eng. J. 227, 151–157.

Xu, M., Xiong, R.H., Li, Y.F., Yang, J.M., Luo, X., Yu, Y.B., Zhao, T.Z.,2010. Pattern transition and holdup behaviors of horizontal oil–water pipe flow. In: 7th International Conference on Multiphase Flow. Tampa, FL, USA, pp. 1–6.